Hindawi Publishing Corporation
International Journal of Antennas and Propagation
Volume 2013, Article ID 106516, 7 pages
http://dx.doi.org/10.1155/2013/106516

Research Article

A Compact Single-Feed Circularly Polarized Microstrip Antenna with Symmetric and Wide-Beamwidth Radiation Pattern

Xihong Ye, Mang He, Pingyuan Zhou, and Houjun Sun

School of Information and Electronics, Beijing Institute of Technology, Beijing 100081, China

Correspondence should be addressed to Mang He; hemang@bit.edu.cn

Received 18 July 2013; Revised 9 October 2013; Accepted 9 October 2013

Academic Editor: Michael Yan Wah Chia

A compact single-feed circularly polarized microstrip antenna is proposed to achieve symmetric radiation pattern over a wide range of observation angles. In order to reduce the radiation aperture and consequently broaden the circular polarization (CP) and the half power beamwidth (HPBW) of the antenna, a partially etched superstrate and a conducting cavity are employed in the design. Further, reasonable axial ratio (AR) and impedance bandwidths are realized within the compact structure by using a simple series crossed-slot aperture coupled feeding. As a consequence, the overall dimension of the fabricated prototype is $0.32\lambda_0 \times 0.32\lambda_0 \times 0.12\lambda_0$ at the center operating frequency of 1.56 GHz, and a 3.0% overlapped bandwidth of 10 dB return loss (RL) and 3 dB AR is obtained. Within the bandwidth, symmetric CP radiation pattern over almost the entire upper hemisphere is observed and the HPBW is also increased from 60° to 106°.

1. Introduction

Microstrip antennas (MSA) are widely used due to the advantages such as low profile, light weight, and easy conformability to host vehicles [1]. In many applications, the requirement of circularly polarized MSA with a wide field of views becomes more demanding in mobile base stations, wide-angle coverage satellite communications, high-resolution radar systems, and so on. For example, a GPS antenna for marine navigation should have good CP performance, adequate gain at low elevation angle, and symmetric and stable radiation at any elevation plane from about 10° above the horizon to the zenith in order to stabilize the receiving signals. As well, compact-size design is often desired in such applications. In general, circular polarization designs can be achieved by using either single or multiple feeding structures [1–9]. For CP antennas of the former type, 3 dB AR beamwidth can be over 60°, but typically the usable overlapped impedance and AR bandwidths are less than 1% [1, 4]. Moreover, due to the inherent asymmetry in the single-feeding structure, symmetric radiation pattern is usually difficult to produce, while, in the latter category, CP radiation is generated by using a relatively complicated feeding network, such as the hybrid or power divider, to enhance the AR bandwidth but at the expense of increased manufacturing cost.

To realize symmetric and wide-beamwidth radiation, extensive researches have been conducted. Duan et al. designed a circular MSA with wide beamwidth by cutting out two symmetrical arc slots and loading three stubs on the circular patch [10]. The method extends the HPBW to 120° effectively, but the antenna is linearly polarized. In [2, 3], a three-layer ground plane (GP) with gradually increased sizes from top to bottom and a pyramid-shape GP were used to broaden the CP beamwidth of MSAs, respectively. However, the use of three-dimensional GP structures increases the profile and lateral sizes of the MSA, which may limit their applications in practicing engineering. In [5–7], the AR bandwidths of MSAs had been extended by using multiple feed techniques, but the HPBW was narrow with the gain at small elevation angle being quite low, which cannot meet the requirements in navigation systems. Moreover, symmetrical radiations on different elevation cuts were not maintained, which may also be a pitfall to avoid in the practical designs. In [8], Nakano et al. utilized a folded conducting wall to partially enclose a probe-fed CP MSA with truncated corners in order to broaden the HPBW to 105° that is approximately 40° wider

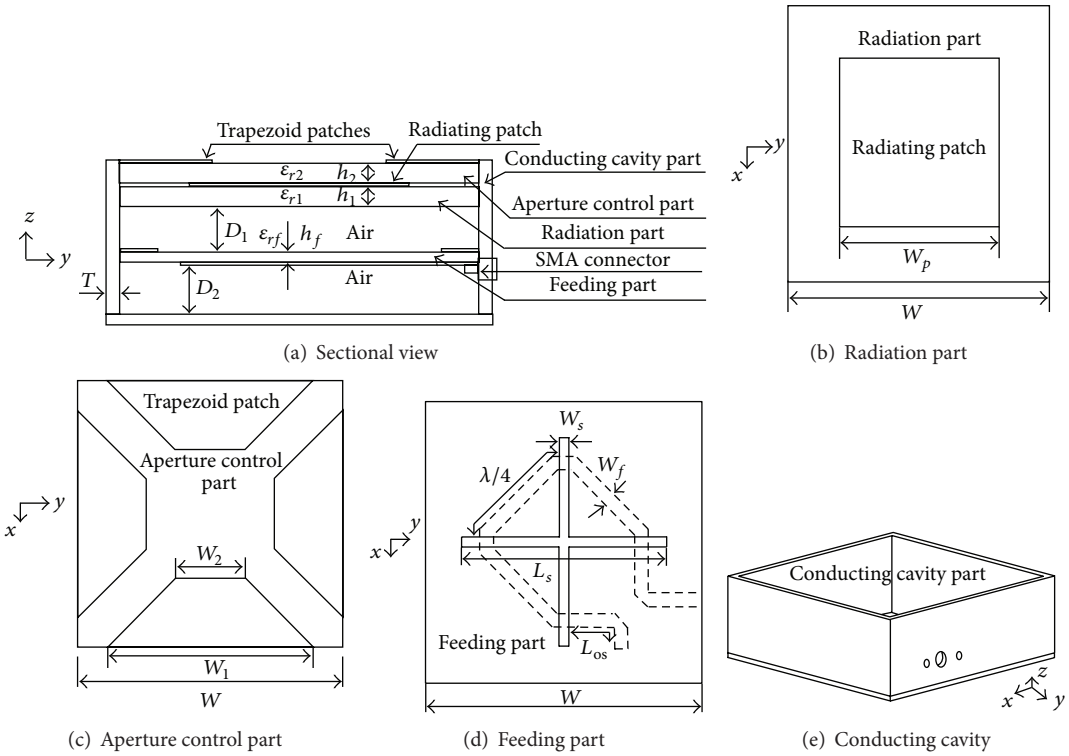

(a) Sectional view (b) Radiation part (c) Aperture control part (d) Feeding part (e) Conducting cavity

Figure 1: Structure of the antenna.

than that of the corresponding conventional MSAs. Also, the patch size is effectively reduced to about $0.372\lambda_0$, that is, only 80% of the MSA without the conducting wall. However, no experimental results and design guidelines were shown. In [9], Kim et al. presented a single-feed MSA with symmetric CP radiation and relatively large bandwidth of 4.6%, but the HPBW was only about 60° and the AR beamwidth was not discussed in that paper. A dual-feed circular patch antenna loaded with curved resonant strips was proposed in [11], and more than 150° 3 dB power and AR beamwidth was achieved at the price of dramatically reduced gain and enlarged lateral sizes ($0.57\lambda_0 \times 0.57\lambda_0$) of the antenna.

In this paper, we present the design of a single-feed compact MSA with symmetric and wide 3 dB AR beamwidth and HPBW in the upper hemisphere. The configuration and design of the antenna is introduced firstly, and then parametric studies are carried out to better understand the design procedure and to optimize the geometrical sizes of the antenna. Finally, a prototype at L band is fabricated and tested, and good agreement is observed between the measured data and the numerical simulations.

2. Antenna Geometry and Design

The configuration of the proposed antenna is shown in Figure 1. It consists of four parts. (1) *The radiation part* (Figure 1(b)) is a square patch of size W_p etched on a square dielectric substrate of permittivity $\varepsilon_{r1} = 2.25$, thickness h_1, and side length W. (2) *The aperture control part* (Figure 1(c)) is formed by four symmetrical 45° isosceles trapezoids of the same size etched on the top surface of a dielectric substrate of permittivity $\varepsilon_{r2} = 2.25$, thickness h_2, and transverse size W. It is mounted on the top of the radiation part as a partially covered superstrate. By adjusting the top and bottom widths W_1 and W_2 of the trapezoids, the radiation aperture can be resized accordingly to control the amount of radiated energy from the patch at the radiation part. Based on our numerical simulations, this aperture control part not only can effectively increase the radiation beamwidth but also can reduce the size of the radiating patch by about 30% even if no dielectric substrate is present. (3) *The feeding part* (Figure 1(d)) consists of a series microstrip feeding line placed behind a crossed-slot with a $\lambda/4$ feeding line positioned between each arm of slot to create the phase quadrature for CP radiation. Thus, the feeding structure has the effect of multiple feed but without complicated external hybrid or power divider. The radiating patch is fed by the feeding part through an air gap of height D_1, and the coupling from the feeding part to the patch can be easily adjusted by changing D_1, the length L_s, and width W_s of the slot. The dielectric constant, thickness, and side length of the substrate to form the feeding part are $\varepsilon_{rf} = 4.4$, h_f, and W, respectively. An open tuning stub of length L_{os} beyond the last arm of the slot is used to achieve impedance matching. (4) *The conducting cavity part* (Figure 1(e)) encompasses the edges and bottom of the former three parts to form a closed radiator as a whole. It is made of brass of thickness $T = 2.0$ mm and the distance between the bottom of the cavity to the feeding layer is D_2. The inner conductor of a coaxial line is soldered to the microstrip line to feed the antenna through the side wall of the cavity, while its outer conductor

Table 1: Optimized dimensions of the proposed antenna (unit: mm).

W	W_1	W_2	W_p	T	h_1	h_2	h_f	D_1	D_2	L_s	W_s	L_{os}	W_f
58.0	45.0	15.0	35.4	2.0	3.16	3.16	1.5	6.5	6.5	44.0	2.0	18.0	2.8

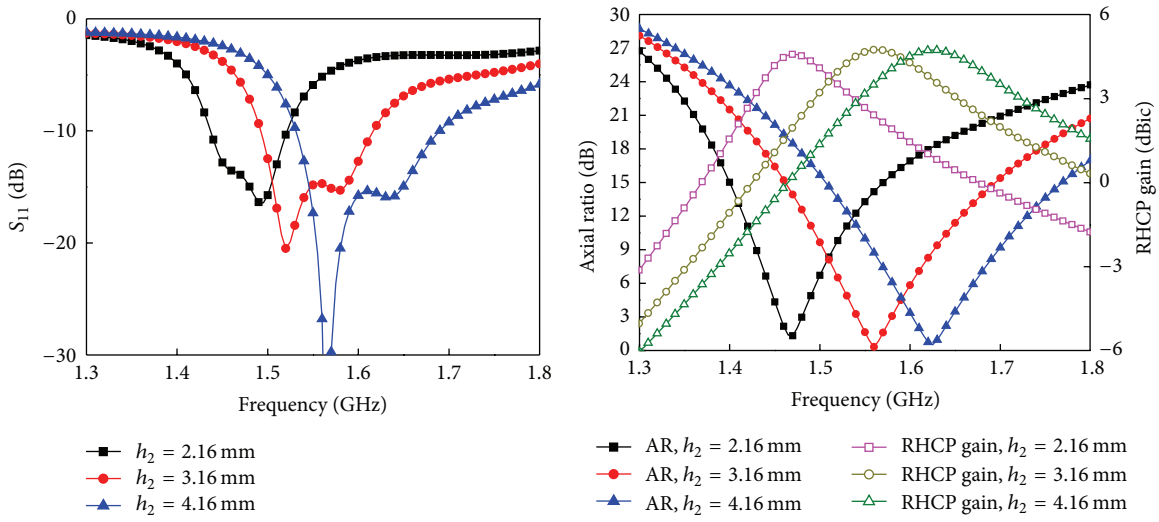

(a) Reflection coefficient S_{11}

(b) AR and RHCP gain

Figure 2: Effect of the aperture control part thickness h_2 on the reflection coefficient, gain, and axial ratio of the antenna.

is connected to an SMA launcher that is mounted on the wall of the cavity.

As an illustration, the antenna is assumed to operate at the center frequency around $f_c = 1.56$ GHz. Due to the existence of the aperture control and conducting cavity parts, the size W_p of the radiating patch can be reduced considerably. In [8], for a vacuum folded conducting wall, the optimum size of the patch for CP radiation is 0.372 wavelengths. Based on this criterion, we can define a size reduction factor SRF to account for the effects of the conducting cavity and aperture control part

$$\text{SRF} = \frac{0.372}{0.5} \cdot \frac{1}{\sqrt{\varepsilon_{\text{reff}}}}, \tag{1}$$

where $\varepsilon_{\text{reff}}$ is the effective permittivity of the dielectric filled in the cavity with the value given by $\varepsilon_{\text{reff}} = (\varepsilon_{r1} + \varepsilon_{r1})/2$. Therefore, W_p can be initially estimated as the product of the conventional size of patch antenna $1/2\lambda_{\text{reff}}$ (λ_{reff} is the wavelength in the dielectric with relative permittivity of $\varepsilon_{\text{reff}}$) and SRF

$$W_p = \frac{\lambda_{\text{reff}}}{2} \cdot \text{SRF} \approx 32\,\text{mm}. \tag{2}$$

The cavity size W is empirically set as double times of W_p

$$W = 2W_p \approx 64\,\text{mm}. \tag{3}$$

With the help of ANSYS HFSS simulator, the optimized parameters of the antenna are summarized in Table 1 for further discussion.

3. Parametric Studies

The effects of some key geometrical sizes on the performance of the proposed CP antenna with right-hand sense are investigated in order to provide useful guidelines in the design. Note that in each parametric study, only one parameter varies and the other parameters remain unchanged in Table 1. Figure 2 shows the effect of the aperture control part thickness h_2 on the reflection coefficient, the right-hand circular polarization (RHCP) gain, and the broadside AR of the antenna. It is seen that the center operating frequency is lowered and the impedance and 3 dB AR bandwidths are reduced when h_2 varies from 4.16 mm to 2.16 mm. The 3 dB AR beamwidth becomes narrow, while the values of RHCP gain and HPBW are only slightly affected by decreasing h_2 as indicated in Table 2.

As stated previously, the sizes of four trapezoids etched from edges of the top surface of the aperture control part can be used to adjust the radiation aperture of the antenna and consequently to change the radiation beamwidth. Figures 3 and 4 show the variations of antenna performance when the bottom and top lengths of the trapezoids W_1 and W_2 vary, respectively, with the base angle of the trapezoid being fixed to 45°. As seen, either an increased size of W_1 or a reduced size of W_2 lowers the operating frequency and decreases the RHCP gain, but at the corresponding center frequency the HPBW of the antenna has only slight variations as listed in Table 2. However, interestingly, the 3 dB AR beamwidth experienced relatively large changes. When the radiation aperture size becomes large by increasing W_2 or decreasing W_1, the 3 dB AR beamwidth is always enhanced. Therefore,

Table 2: The effects of parameters h_2, W_1, W_2, and D_1 on the center operating frequency, HPBW, and 3 dB beamwidth of the antenna.

Performance	h_2 (mm)			W_1 (mm)			W_2 (mm)			D_1 (mm)		
	2.16	3.16	4.16	40	45	50	10	15	20	5.5	6.5	7.5
f_c (GHz)	1.47	1.56	1.63	1.735	1.56	1.44	1.46	1.56	1.71	1.58	1.56	1.55
RHCP gain (dBic)	4.72	4.74	4.74	5.01	4.74	4.36	4.46	4.74	4.95	4.76	4.74	4.63
HPBW (°)	−55–55	−55–55	−55–55	−53–53	−55–55	−56–56	−56~56	−55~55	−54~53	−55~55	−55~55	−54~53
3 dB AR coverage (°)	−86–86	−96–97	−99–99	−105–105	−96–97	−82–82	−87~87	−96~97	−103~103	−94~94	−96~97	−94~95

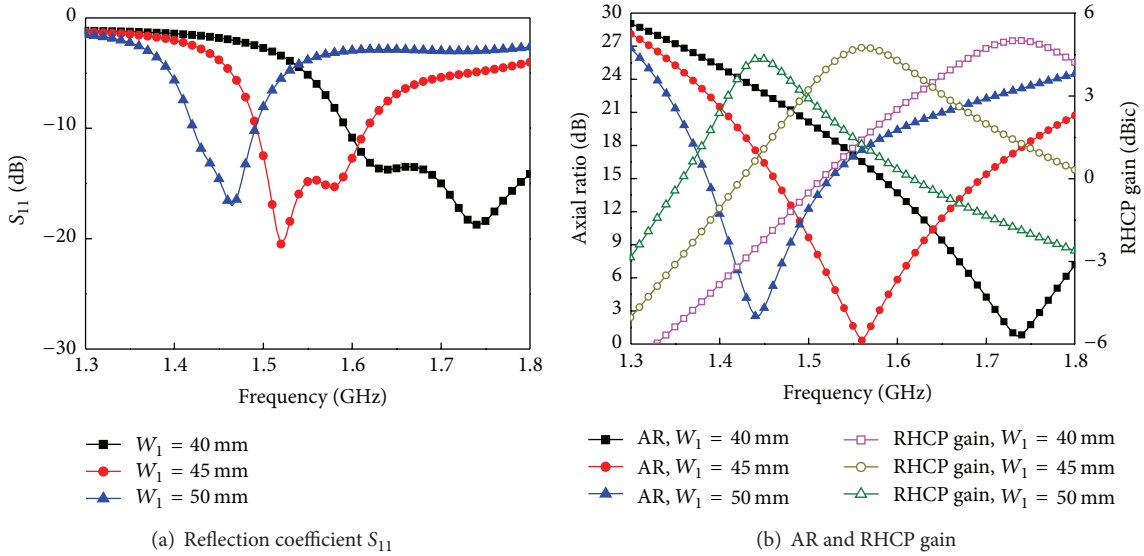

(a) Reflection coefficient S_{11}

(b) AR and RHCP gain

Figure 3: Effect of the bottom length W_1 of the trapezoid on the reflection coefficient, gain, and axial ratio of the antenna.

we can achieve the desirable radiation properties effectively by adjusting the parameters of the aperture control part.

In Figure 5, the effect of the height of the air gap D_1 between the radiation part and feeding part on the antenna's characteristics is shown. It is seen that when D_1 is decreased the impedance bandwidth is enhanced but the CP radiation is degraded clearly. On the other hand, if the value of D_1 is too large, both the impedance and AR bandwidth will be deteriorated and the RHCP gain will be reduced due to the weak coupling between the feeding and the radiation structures. In summary, the effects of the important parameters h_2, W_2, W_1, and D_1 on the center operating frequency, the maximum value of RHCP gain, HPBW, and 3 dB AR beamwidth of the antenna are listed in Table 2.

4. Measured Results and Discussion

Figures 6(a) and 6(b) show the fabricated RHCP antenna with the center frequency being around 1.56 GHz. Its overall dimensions are 62 mm × 62 mm × 22.82 mm ($0.32\lambda_0 \times 0.32\lambda_0 \times 0.12\lambda_0$ at 1.56 GHz). The antenna test system includes a vector network analyzer (VNA) HP8510C, a one-dimensional rolling-plane antenna test turntable, and two L band standard horn antennas. All measurements were carried out in an anechoic chamber. The reflection coefficient measured by the VNA is shown in Figure 7. It is seen that the 10 dB RL bandwidth is about 6.8% (1.495–1.60 GHz), which is slightly narrower than the simulated results. The small discrepancy may be caused by the miss match from the SMA connector and uncertainty of the dielectric materials used in the fabrication.

The photograph of radiation pattern measurement is shown in Figure 6(c), in which the fabricated antenna was used as the transmitting antenna while the standard horn antennas were used as the receiving antennas. The horn antenna was rotated around its axis and the maximum and minimum received power $P_{\max}$ and $P_{\min}$ were recorded by the VNA, and then the value of AR in decibel can be directly obtained by AR = $P_{\max} - P_{\min}$. The CP radiation pattern of the antenna can also be obtained by using the existing test system and the following equations:

$$\begin{aligned} (2E_L)^2 &= E_{1m}^2 + E_{2m}^2 - 2E_{1m}E_{2m}\cos(270^\circ - \Delta\varphi_l), \\ (2E_R)^2 &= E_{1m}^2 + E_{2m}^2 - 2E_{1m}E_{2m}\cos(\Delta\varphi_l - 90^\circ), \end{aligned} \tag{4}$$

where E_{1m} and E_{1m} are magnitudes of two orthogonal linearly polarized electric field components with a phase difference $\Delta\varphi_l$ between them and E_L and E_R are magnitudes of the LHCP and RHCP components, respectively. If the received power and the phase of two linear polarization components at E- and H-planes of the standard horn antenna

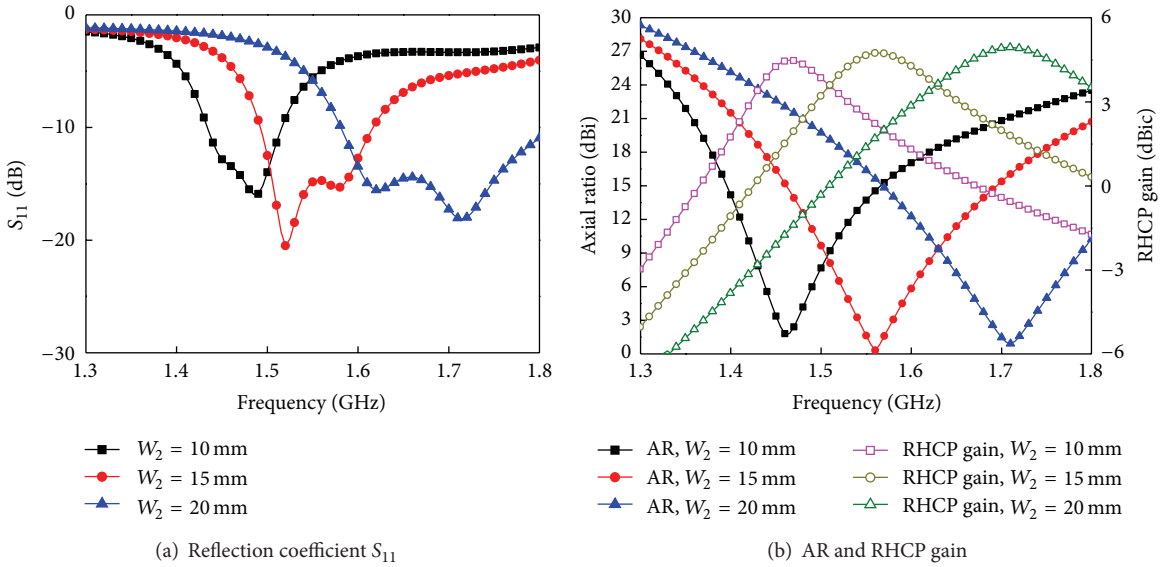

(a) Reflection coefficient S_{11} (b) AR and RHCP gain

FIGURE 4: Effect of the top length W_2 of the trapezoid on the reflection coefficient, gain, and axial ratio of the antenna.

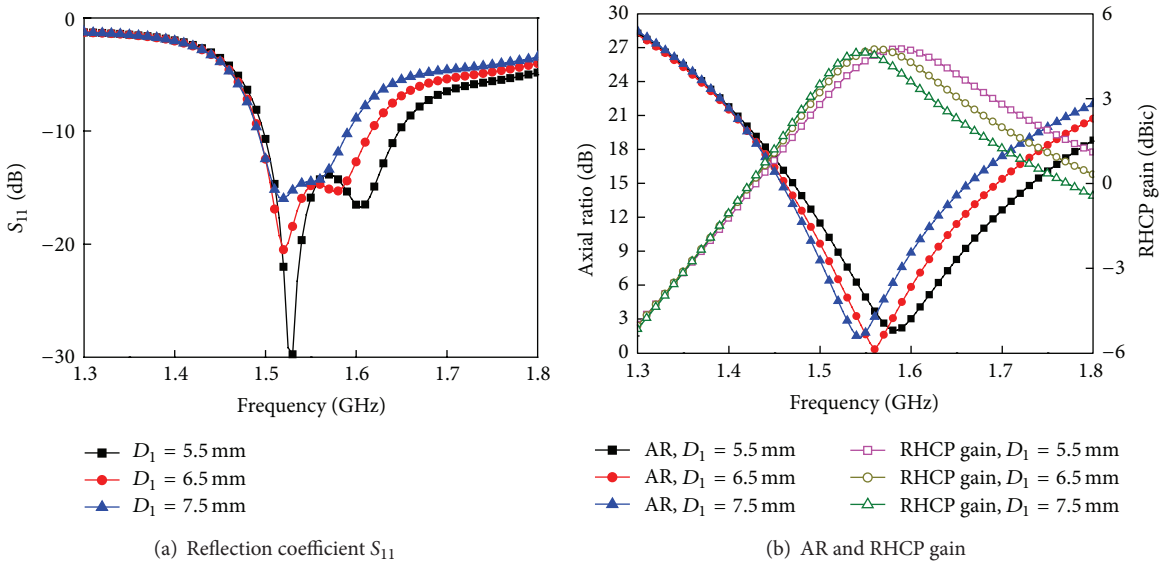

(a) Reflection coefficient S_{11} (b) AR and RHCP gain

FIGURE 5: Effect of the height of air gap D_1 on the reflection coefficient, gain, and axial ratio of the antenna.

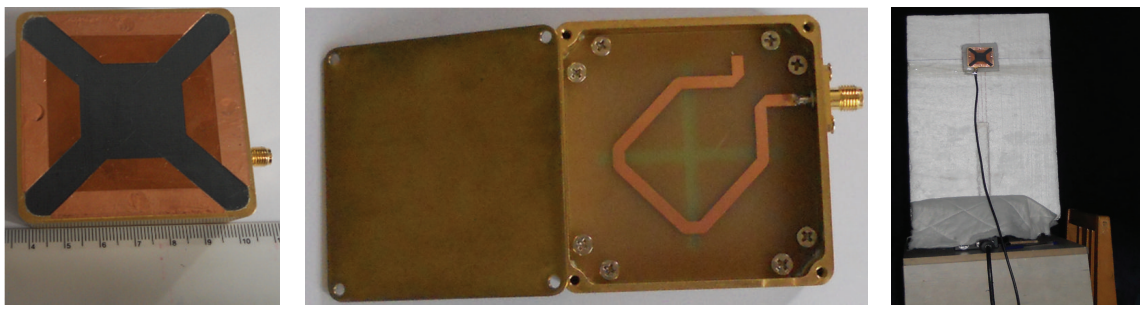

(a) (b) (c)

FIGURE 6: (a) top View; (b) bottom View; (c) radiation pattern measurement.

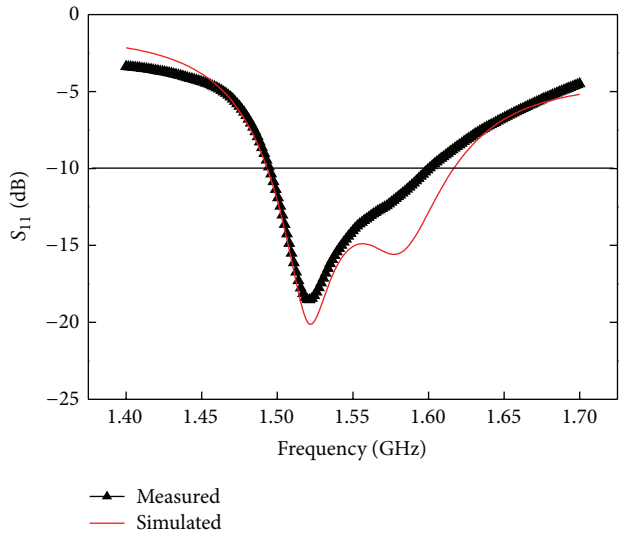

Figure 7: Measured and simulated reflection coefficient of the fabricated antenna.

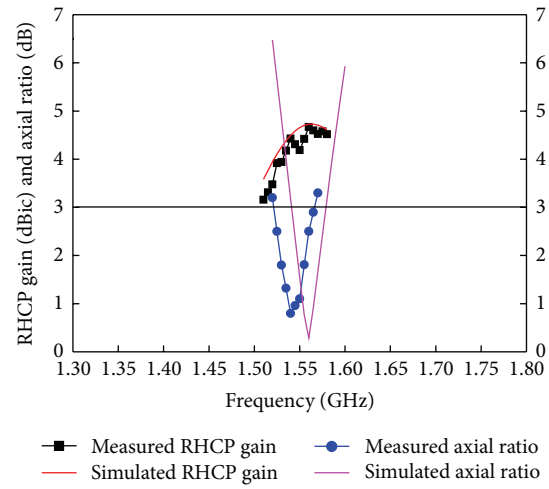

Figure 8: Measured and simulated RHCP gain and axial ratio of the fabricated antenna.

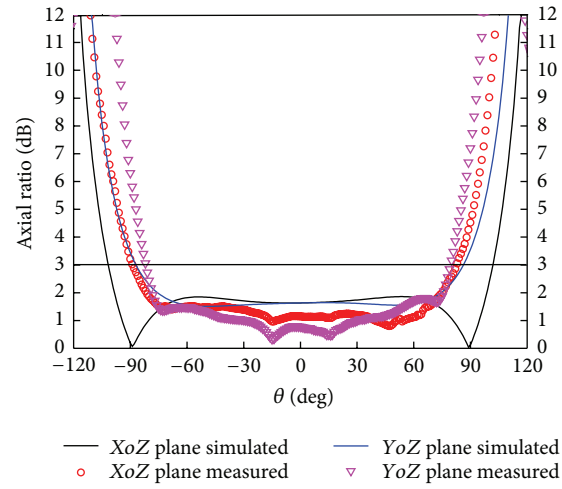

Figure 9: Measured and simulated axial ratio spatial distribution at 1.55 GHz.

are P_e, φ_e, P_h and φ_h, respectively, then the LHCP and RHCP components can be expressed as

$$4P_L = P_e + P_h - 2\sqrt{P_e P_h}\cos\left(270^\circ - \Delta\varphi\right),$$
$$4P_R = P_e + P_h - 2\sqrt{P_e P_h}\cos\left(\Delta\varphi - 90^\circ\right), \quad (5)$$
$$\Delta\varphi = \varphi_e - \varphi_h.$$

To get RHCP gain of the antenna, two standard horn antennas must be used. First, the fabricated antenna is used as the transmitting antenna and one of the horn antennas is used as the receiving antenna, and then we obtain a set of the received power and phase of the signal P_{e0}, φ_{e0}, P_{h0}, and φ_{h0}. Next, we got another set of P_{e1}, φ_{e1}, P_{h1}, and φ_{h1} using the other horn antenna in place of the fabricated antenna as the transmitting antenna. So we could calculate the RHCP gain by using the comparison method and (5).

Figure 8 shows the measured RHCP gain and axial ratio at broadside direction versus frequency. The measured 3 dB AR bandwidth is 3.0% (1.520–1.567 GHz), and the frequency with minimum AR is 1.544 GHz, that is, about 1% lower than the simulated one. The difference between the measured and simulated RHCP gain is less than 0.5 dB over the entire frequency band. It is seen that the measured gain follows the simulation, while there is a small frequency shift between the measured and simulated AR. We think that this discrepancy is due to the alignment of the transmitting and receiving antennas during the gain measurement since the measurement should be carried out two times by using the fabricated antenna as the receiving antenna first and again the standard horn antenna, while in the AR measurement only one receiving antenna is needed, which will lead to a small frequency shift between the measured gain and AR. Figures 9 and 10 depict the spatial distribution of axial ratio and the normalized radiation pattern at 1.55 GHz, respectively. The radiation pattern exhibits excellent stability with respect to the azimuthal angle φ, and good symmetry is also observed in the elevation planes. The average measured HPBW in XoZ ($\varphi = 0^\circ$) and YoZ ($\varphi = 90^\circ$) planes is 106°, and the 3 dB AR beamwidth nearly covers the entire upper half space (±80°). As seen in Figures 9 and 10, the measured cross-polarization component at low elevation angle is higher than the simulated results, which may be due to the influence of the feeding coaxial line. For comparison purpose, the measured and simulated data of the return loss and axial ratio versus frequency are listed in Table 3, while the HPBW and 3 dB AR spatial coverage at 1.55 GHz are shown in Table 4.

5. Conclusion

A compact CP MSA with wide 3 dB power and axial ratio beamwidth and reasonable bandwidth is realized by the combined use of a partially covered superstrate, a conducting cavity, and a single-feed aperture coupled patch antenna

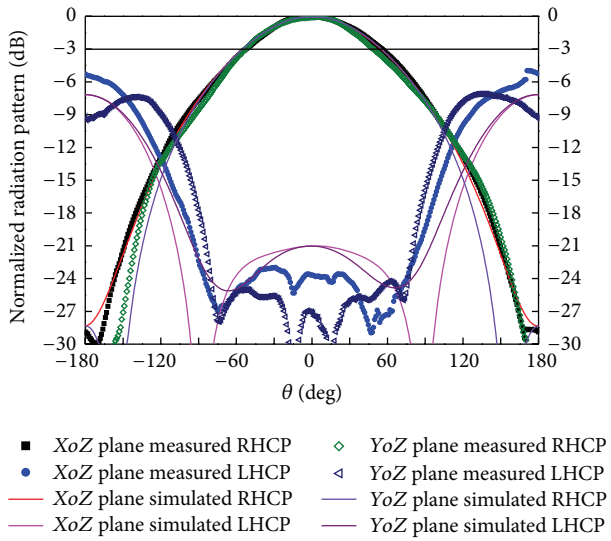

Figure 10: Measured and simulated radiation patterns at 1.55 GHz.

Table 3: Measured and simulated 10 dB RL and 3 dB AR frequency range and bandwidths.

	frequency range (GHz)	f_c (GHz)	BW (%)
10 dB RL			
Measured	1.495–1.600	1.548	6.80
Simulated	1.494–1.616	1.555	7.80
3 dB AR			
Measured	1.520–1.567	1.544	3.04
Simulated	1.541–1.579	1.560	2.40

Table 4: Measured and simulated HPBW and 3 dB AR coverage at 1.55 Ghz.

	$\varphi = 0^\circ$	$\varphi = 45^\circ$	$\varphi = 90^\circ$	$\varphi = 135^\circ$
HPBW (°)				
Measured	−53–56	—	−53–50	—
Simulated	−55–55	−56–56	−55–55	−56–56
3 dB AR coverage (°)				
Measured	−89–83	—	−80–79	—
Simulated	−101–101	−92–92	−88–88	−92–92

without using any complicated power divider. The overall dimension of the antenna is as small as $0.32\lambda_0 \times 0.32\lambda_0 \times 0.12\lambda_0$, and the radiating patch size is only $0.19\lambda_0$, that is, nearly half of the antennas in the existing literature [8, 9]. The overlapped 10 dB return loss and 3 dB axial ratio bandwidth is 3%, which is quite satisfactory when considering a single-feed MSA of such compact size. By using the aperture control part, the proposed antenna achieves very symmetrical and stable CP radiation almost in the entire upper hemisphere, and the average HPBW is about 106° that is also much wider than that of the conventional MSA. Although only a RHCP MSA operating at L band is considered in this paper, the design methodology can also be used to design LHCP MSAs in other bands.

Conflict of Interests

The authors declare that there is no conflict of interests regarding the publication of this paper.

References

[1] K.-L. Wong, *Compact and Broadband Microstrip Antennas*, Wiley, New York, NY, USA, 2002.

[2] C.-L. Tang, J.-Y. Chiou, and K.-L. Wong, "Beamwidth enhancement of a circularly polarized microstrip antenna mounted on a three-dimensional ground structure," *Microwave and Optical Technology Letters*, vol. 32, no. 2, pp. 149–153, 2002.

[3] C.-W. Su, S.-K. Huang, and C.-H. Lee, "CP microstrip antenna with wide beamwidth for GPS band application," *Electronics Letters*, vol. 43, no. 20, pp. 1062–1063, 2007.

[4] P. C. Sharma and K. C. Gupta, "Analysis and optimized design of single feed circularly polarized microstrip antennas," *IEEE Transactions on Antennas and Propagation*, vol. AP-31, no. 6, pp. 949–955, 1983.

[5] K.-L. Wong and T.-W. Chiou, "Broad-band single-patch circularly polarized microstrip antenna with dual capacitively coupled feeds," *IEEE Transactions on Antennas and Propagation*, vol. 49, no. 1, pp. 41–44, 2001.

[6] C. Lin, F.-S. Zhang, Y.-C. Jiao, F. Zhang, and X. Xue, "A three-fed microstrip antenna for wideband circular polarization," *IEEE Antennas and Wireless Propagation Letters*, vol. 9, pp. 359–362, 2010.

[7] L. Bian, Y. X. Guo, L. C. Ong, and X. Q. Shi, "Wideband circularly-polarized patch antenna," *IEEE Transactions on Antennas and Propagation*, vol. 54, no. 9, pp. 2682–2686, 2006.

[8] H. Nakano, S. Shimada, J. Amauchi, and M. Miyata, "A circularly polarized patch antenna enclosed by a folded conducting wall," in *Proceedings of the IEEE Topical Conference on Wireless Communication Technology*, pp. 134–135, 2003.

[9] H. Kim, B. M. Lee, and Y. J. Yoon, "A single-feeding circularly polarized microstrip antenna with the effect of hybrid feeding," *IEEE Antennas and Wireless Propagation Letters*, vol. 2, pp. 74–77, 2003.

[10] Z.-S. Duan, S.-B. Qu, Y. Wu, and J.-Q. Zhang, "Wide bandwidth and broad beamwidth microstrip patch antenna," *Electronics Letters*, vol. 45, no. 5, pp. 249–251, 2009.

[11] W. Q. Cao, B. N. Zhang, A. J. Liu et al., "A low-profile CP microstrip antenna with broad beamwidth based on loading with curved microstrip resonant structures," *Journal of Electromagnetic Waves and Applications*, vol. 26, no. 11-12, pp. 1602–1610, 2012.